Journal of Thermal Analysis and Calorimetry, Vol. 81 (2005) 511–521

SUCCESSIVE PHASE TRANSITIONS OF *p*-METHYLBENZYL ALCOHOL CRYSTAL STUDIED BY X-RAY AND ADIABATIC CALORIMETRY
Structural disorder in room-temperature phase

Hideki Saitoh[1], *Satoaki Ikeuchi*[2] *and Kazuya Saito*[3]*

[1]Molecular Analysis and Life Science Center, Saitama University, 255 Shimo-okubo, Sakura-ku, Saitama 338-8570, Japan
[2]Research Center for Molecular Thermodynamics,Graduate School of Science, Osaka University, Toyonaka, Osaka 560-0043, Japan
[3]Department of Chemistry, Graduate School of Pure and Applied Sciences, University of Tsukuba, Tsukuba, Ibaraki 305-8571, Japan

Crystal structures of the room-temperature (RT) and low-temperature (LT) phases of *p*-methylbenzyl alcohol were reexamined by single-crystal X-ray diffraction method while paying special attention to detect structural disorder in the RT phase involved in successive structural phase transitions at 179 and 210 K. In the RT phase at 250 K, positional disorder of oxygen atoms was detected in contrast to the previous structure report. The structure of the LT phase coincided to the previous one. Heat capacities were measured by adiabatic calorimetry below 350 K, which covers the structural phase transitions and fusion at 331.87 K. The structural phase transitions were of first-order and required long time for completion. The combined magnitude of entropies of transition was ca. 5 J K^{-1} mol^{-1}, a part of which can be ascribed to the positional disorder observed in the structure analysis. Standard thermodynamic functions are tabulated below 350 K.

Keywords: *adiabatic calorimetry, crystal structure, heat capacitie, order-disorder, phase transition, p-methylbenzyl alcohol, thermodynamic functions, X-ray diffraction*

Introduction

Crystals of *p*-halogeno-substituted benzyl alcohol (abbreviated as *p*-XBA : *X*=Cl, Br) consist of one-dimensional chain of molecules [1, 2]. The molecules are related by a screw axis, and connected by hydrogen-bonds. The hydrogen atoms in hydrogen bonds are reported to locate at one side of the bond. Around 200 K, crystals of *p*-XBA undergo phase transitions without changes in both space group and unit cell [1–5]. The existing structure reports claim that the direction of the hydrogen-bonds is reversed upon the phase transition with a shift of the oxygen atom in the OH group. This inversion accompanies that of the polarization. Indeed, anomalous behavior was reported in dielectric constant [5].

The crystal of the title compound, *p*-methylbenzyl alcohol (*p*-MBA), has the same characteristics to halogeno compounds with some complexity [6]. There are two types of chains. Chain B consists of molecules B (after the existing structure report) related by a screw axis. The other consists of two non-equivalent molecules A and C (chain A–C). Although there is no exact screw axis along the center of the chain A–C, the molecular packing in the chain is close to the chain B. The molecular packing in the chains is opposing between the chain B and A–C. The polarizations are anti-parallel to each other, accordingly. In spite of this slight complexity in the crystal structure, the crystal of *p*-MBA is reported to undergo successive phase transitions at 211 and 172 K similarly to *p*-XBA. The location of the hydrogen atoms in the hydrogen bonds is essentially the same in the chains B and A–C at room temperature (RT). In the low temperature (LT) phase, the direction of the hydrogen bonds is reversed in both chains.

Hashimoto *et al*. [1–6] have conducted extensive studies on phase transitions in *p*-MBA and *p*-XBA utilizing crystallography, dielectric measurements, nuclear magnetic resonance (NMR) of ^{2}D nuclei, nuclear quadrupole resonance (NQR) of halogen nucleus as briefly summarized above. They reported that the temperature dependence of T_1, nuclear relaxation time, was well described by assuming the nuclear dynamics in a double-well potential well. Although the presence of double-well potential itself can easily be imagined for hydrogen-bonds, it also suggests an order-disorder mechanism for the successive phase transitions. In this context, their analyses on experimental results seem to lack the consistency. Besides, they reported that the phase transition behavior exhibits some history dependence. This situation prompted the authors to start the reexamination of crystal structures of *p*-MBA to see possible disorder in the RT

* Author for correspondence: kazuya@chem.tsukuba.ac.jp

1388–6150/$20.00

Akadémiai Kiadó, Budapest, Hungary
Springer, Dordrecht, The Netherlands

Table 1 Experimental conditions and crystallographic parameters

Chemical formula	$C_8H_{10}O$	
Formula Mass	122.16	
T/K	250(1)	100(1)
Crystal size/mm	0.40·0.20·0.15	0.36·0.22·0.12
Wavelength/Å	0.71073	
Crystal system	Monoclinic	
Space group	$P2_1$	
a/Å	14.5892(14)	14.5559(11)
b/Å	4.9483(5)	4.8495(3)
c/Å	15.0417(15)	15.0050(11)
b/°	105.812(2)	107.1380(10)
V/Å^3	1044.80(18)	1012.16(12)
Z	6	
F(000)	396	
D_x / Mg·m^{-3}	1.165	1.202
μ/mm^{-1}	0.075	0.078
Absorption correction	Empirical (SADABS [8])	
T_{max} and T_{min}	0.9888, 0. 9706	0.9908, 0.9726
θ_{max}/°	28.89	27.86
Index ranges	$-16 \leq h \leq 19$	$-19 \leq h \leq 19$
	$-6 \leq k \leq 6$	$-6 \leq k \leq 5$
	$-19 \leq l \leq 19$	$-19 \leq l \leq 17$
No. of reflections collected	7754	7353
No. of independent reflections	4172 [*R*(int)=0.0211]	4307 [*R*(int)=0.0184]
Completeness	100.0% [θ ≤27.89°]	99.9% [θ ≤27.86°]
No. of reflections [I > 2σ(I)]	2904	3976
Refinement method	Full-matrix least-squares on F^2	
H-atom parameters	Refined all	
Refinement assuming non-split O *atoms*		
No. of data used in refinement	4172	4307
No. of parameters	364	364
$R[F^2>2\sigma(F^2)]$	0.0614	0.0447
c_1 and c_2 (*)	0.0881, 0.1599	0.0805, 0.0627
$wR(F^2)$	0.1763	0.1190
S	1.031	1.040
$(\Delta/\sigma)_{max}$	< 0.001	< 0.001
$\Delta\rho_{max}$ and $\Delta\rho_{min}$/e Å^{-3}	0.340, –0.251	0.368, –0.248
Refinement assuming split O *atoms*		
No. of data used in refinement	4172	
No. of parameters	389	
$R[F^2>2\sigma(F^2)]$	0.0554	
c_1 and c_2 (*)	0.0825, 0.0643	
$wR(F^2)$	0.1562	
S	1.018	
$(\Delta/\sigma)_{max}$	0.001	
$\Delta\rho_{max}$ and $\Delta\rho_{min}$/e Å^{-3}	0.172, –0.174	

(*) $w = 1 / [\sigma^2(F_0^2) + (c_1 \cdot P)^2 + c_2 \cdot P]$ where $P = (F_0^2 + 2F_c^2) / 3$

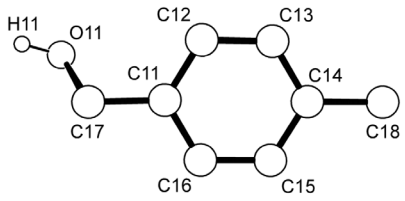

Fig. 1 Numbering scheme of atoms in a *p*-methylbenzyl alcohol molecule

phase and the precise adiabatic calorimetry to observe the equilibrium phase transition behavior and to determine the entropies of transition.

Experimental

X-ray diffraction

The reagent was purchased from Wako Pure Chemical Industries, Ltd. The crystal used for the measurements was selected from the reagent without purification and recrystallization. All X-ray measurements were made using a diffractometer SMART APEX (Bruker AXS K.K.) equipped with a refrigerator by streaming cold nitrogen gas (Cryostream cooler, Oxford Cryosystems). The data collection was performed at 250 K for the RT phase to reduce the effects of sublimation of the sample at room temperature. The data collection was performed at 100 K for the LT phase. Unit-cell refinement and data reduction were carried out by SAINT and SADABS programs [7, 8]. Program used to solve and refine structures was SHELXTL [9]. Ortep-3 for Windows was used to produce crystal-structure illustrations [10]. The experimental conditions and the crystallographic parameters are tabulated in Table 1. The atomic numbering scheme is shown in Fig. 1.

Adiabatic calorimetry

Commercial reagent (Tokyo Chemical Industry, Co., Ltd.) was purified by fractional sublimation at 30°C in vacuum. The purified specimen was crushed gently and loaded into a gold-plated copper calorimeter vessel, which was pinched off after introducing helium gas (10^5 Pa at room temperature) to assist thermal uniformity inside the vessel. Mass of the sample loaded was 1.8460 g (15.111 mmol) after the buoyancy correction. The contribution of the sample to the total heat capacity including those of the vessel and helium gas was 23% at 50 K, 19% at 100 K, 22% at 200 K, 26% at 300 K and 35% at 350 K.

Chemical analysis of the purified specimen yielded the following results: C 78.26% (calcd. 78.65%) and H 8.24% (8.25%). The purity of the sample used for the calorimetry was determined to be 99.95 mol% by the cryometry as described later.

The thermometer attached to the calorimeter vessel is a platinum resistance thermometer (MINCO, S1059). Its temperature scale is based upon the ITS-90. The calorimetric measurement was performed by using a laboratory-made adiabatic calorimeter, the details of which was described elsewhere [11].

Results and discussion

Crystal structure of RT phase

The crystal structure of *p*-methylbenzyl alcohol at 250 K in the room-temperature phase was essentially the same as the previous report [6]. In this study, however, it was found that the thermal ellipsoids of O31 and C37 atoms in the molecule C were larger than those of O11 and O21 in the molecule A and B, and then a remarkable peak of electron density was found close to the O31 atom in molecule C in the difference Fourier synthesis map (D-map). This electron peak was identified another site of the O31 atom. The structure refinement assuming the disorder of the O31 atom (split-atom analysis) was converged successfully with electron density peaks near by the O21 and O11 atoms on the D-map. Finally, the O31, O21 and O11 atoms were successfully split into two sites for each. The thermal displacement parameter of the O11B atom was put to be isotropic in the refinement. The positional and thermal parameters obtained by the split-atom analysis are tabulated in Table 2. The crystal structure obtained by this analysis viewed along the *b*-axis is shown in Fig. 2. The site occupancy of an O atom in one side was determined as ca. 54(6)% for molecule C, 62(9)% for B, 5(2)% for A. However, these occupancies depended on the condition used for the refinement, as to whether the thermal parameters of each additional O atom were set as isotropic or anisotropic. No positional disorder of the H atoms on –OH groups is detected within the experimental precision and the directions of –OH groups are the same as the previous report [6]. Lengths and angles of hydrogen bond obtained by the split O atom refinement are tabulated in Table 3. These are in the range of typical value except for some hydrogen bonds related to the O11B atom. It is found that the O11A-H11···O31B bond is shorter than the O11A-H11···O31A bond and the O31A-H31···O11A bond angle is wider than the O31B-H31···O11A bond one. For the molecule C in the hydrogen-bond chain of molecule A–C–A–C–, it is suggested that there exist two stable conformations, which are favorable to upward and downward hydrogen bond, respectively.

Table 2 Atomic coordinates and thermal parameters of room-temperature phase of *p*-methyl benzyl alcohol at 250 K obtained by the split atom analysis

Atom	*x*	*y*	*z*	U_{eq}	Occupancy
C11	0.85083(15)	–0.0190(6)	0.14122(18)	0.0433(6)	1
C12	0.88973(19)	0.0734(7)	0.23079(18)	0.0496(7)	1
C13	0.96293(18)	0.2606(7)	0.25035(19)	0.0504(7)	1
C14	0.99962(17)	0.3624(7)	0.18150(18)	0.0461(6)	1
C15	0.96072(18)	0.2728(7)	0.09311(19)	0.0504(7)	1
C16	0.88750(19)	0.0860(7)	0.07273(18)	0.0499(7)	1
C17	0.7743(2)	–0.2274(7)	0.1172(3)	0.0570(9)	1
C18	1.0781(2)	0.5710(7)	0.2023(3)	0.0581(8)	1
O11A	0.7008(2)	–0.1666(5)	0.1576(4)	0.0604(14)	0.946(15)
O11B	0.690(2)	–0.184(9)	0.106(4)	0.044(13)	0.054(15)
C21	0.68468(16)	0.8483(7)	0.47154(17)	0.0433(6)	1
C22	0.72554(19)	0.7535(7)	0.55989(18)	0.0515(7)	1
C23	0.79836(19)	0.5637(7)	0.57587(19)	0.0529(8)	1
C24	0.83332(16)	0.4676(6)	0.50530(19)	0.0471(7)	1
C25	0.79116(19)	0.5660(7)	0.41683(19)	0.0512(7)	1
C26	0.71834(18)	0.7513(7)	0.40100(18)	0.0514(7)	1
C27	0.6065(2)	1.0575(7)	0.4526(2)	0.0564(8)	1
C28	0.9117(2)	0.2617(9)	0.5224(3)	0.0673(10)	1
O21A	0.5483(14)	1.010(4)	0.5128(14)	0.064(4)	0.38(9)
O21B	0.5381(12)	1.0099(17)	0.495(2)	0.067(3)	0.62(9)
C31	0.47521(17)	0.4836(7)	0.18167(19)	0.0506(7)	1
C32	0.4289(2)	0.5870(7)	0.09699(19)	0.0553(8)	1
C33	0.35695(19)	0.7739(7)	0.08855(19)	0.0558(8)	1
C34	0.32966(16)	0.8645(6)	0.16377(18)	0.0457(6)	1
C35	0.37626(19)	0.7593(7)	0.24825(19)	0.0544(7)	1
C36	0.4488(2)	0.5728(7)	0.25789(19)	0.0556(8)	1
C37	0.5526(3)	0.2747(9)	0.1960(3)	0.0782(12)	1
C38	0.2514(2)	1.0694(7)	0.1538(3)	0.0615(9)	1
O31A	0.6105(9)	0.328(2)	0.1394(8)	0.042(3)	0.46(6)
O31B	0.6291(16)	0.346(3)	0.172(3)	0.101(5)	0.54(6)
H11	0.671(3)	–0.303(8)	0.157(3)	0.085(13)	1
H12	0.8646(17)	–0.005(8)	0.2822(17)	0.067(8)	1
H13	0.983(2)	0.321(10)	0.308(2)	0.092(11)	1
H15	0.9838(17)	0.342(8)	0.0448(15)	0.061(8)	1
H16	0.8645(15)	0.042(6)	0.0118(15)	0.044(7)	1
H171	0.803(2)	–0.377(8)	0.157(2)	0.072(10)	1
H172	0.753(2)	–0.253(9)	0.051(2)	0.112(13)	1
H181	1.061(2)	0.754(8)	0.222(2)	0.087(10)	1
H182	1.116(3)	0.530(14)	0.262(3)	0.151(19)	1
H183	1.116(2)	0.545(9)	0.1653(19)	0.075(10)	1
H21	0.508(3)	1.157(8)	0.493(2)	0.062(10)	1
H22	0.7030(15)	0.810(7)	0.6076(15)	0.045(6)	1
H23	0.8331(17)	0.531(7)	0.6425(16)	0.058(8)	1
H25	0.8149(19)	0.503(8)	0.3662(18)	0.077(9)	1
H26	0.6882(18)	0.829(8)	0.3343(18)	0.075(9)	1

Table 2 Continued

Atom	*x*	*y*	*z*	U_{eq}	Occupancy
H271	0.567(2)	1.050(7)	0.3847(19)	0.076(9)	1
H272	0.6355(15)	1.245(6)	0.4623(15)	0.039(6)	1
H281	0.887(2)	0.087(8)	0.5195(19)	0.068(9)	1
H282	0.949(3)	0.267(13)	0.485(3)	0.138(18)	1
H283	0.963(3)	0.303(11)	0.578(2)	0.110(13)	1
H31	0.643(3)	0.224(8)	0.147(3)	0.086(15)	1
H32	0.448(2)	0.538(9)	0.0412(19)	0.084(10)	1
H33	0.3326(19)	0.860(8)	0.0349(19)	0.075(10)	1
H35	0.3603(18)	0.836(8)	0.3000(17)	0.066(8)	1
H36	0.477(2)	0.527(8)	0.3150(19)	0.079(10)	1
H371	0.526(3)	0.202(9)	0.135(2)	0.111(16)	1
H372	0.544(3)	0.118(10)	0.219(3)	0.108(14)	1
H381	0.272(3)	1.239(11)	0.154(3)	0.119(16)	1
H382	0.209(3)	1.048(13)	0.099(3)	0.141(19)	1
H383	0.222(2)	1.073(10)	0.202(2)	0.090(11)	1

Table 3 Hydrogen bonds in room-temperature phase of *p*-methylbenzyl alcohol at 250 K in split-atom refinement /Å

D–H...A	*d*(D–H)	*d*(H...A)	*d*(D...A)	∠DHA
O31A–H31...O11A	0.69(4)	2.09(4)	2.756(12)	161(5)
O31A–H31...O11B	0.69(4)	2.27(7)	2.89(5)	150(5)
O31B–H31...O11A	0.77(5)	2.09(4)	2.777(14)	148(5)
O31B–H31...O11B	0.77(5)	2.27(7)	3.03(6)	167(5)
O21A–H21...O21A_#1	0.93(4)	1.92(4)	2.821(19)	162(3)
O21A–H21...O21B_#1	0.93(4)	1.90(4)	2.76(2)	154(3)
O21B–H21...O21A_#1	0.85(4)	1.92(4)	2.76(2)	174(4)
O21B–H21...O21B_#1	0.85(4)	1.90(4)	2.732(8)	169(4)
O11A–H11...O31A_#2	0.80(4)	2.01(4)	2.807(12)	169(4)
O11A-H11...O31B_#2	0.80(4)	1.87(4)	2.661(13)	167(4)
O11B–H11...O31A_#2	1.06(6)	2.01(4)	2.79(4)	127(4)
O11B–H11...O31B_#2	1.06(6)	1.87(4)	2.77(4)	140(5)

Symmetry transformations used to generate equivalent atoms: #1 $-x+1, y+1/2, -z+1$; #2 $x, y-1, z$

Crystal structure of LT and IT phases

The crystal structure of the LT phase at 100 K is essentially the same as that at 120 K reported previously [6]. The positional and thermal parameters at 100 K are tabulated in Table 4. The thermal ellipsoids of all non-hydrogen atoms have usual magnitude. There is no disorder and the directions of hydrogen-bond chains of –OH groups in the LT phase are reversed with respect to those in the RT phase. Lengths and angles of hydrogen bond are tabulated in Table 5. It is found that the angles of these hydrogen bonds in the LT phase become smaller than those in the RT. It suggests that the hydrogen-bond interaction was more dominant for the molecular packing in the LT phase.

Preliminary experiments on the structure of the IT phase showed that the structure is similar to that of the LT phase. A residual peak suggesting the presence of disorder was detected in the D-map only around the O31 atom in the molecule C. Attempt to establish the structure of the IT phase was not made because it requires a long time for stabilization at low temperature, as shown in the following result of adiabatic calorimetry.

Fusion and cryometry on calorimetric sample

p-MBA melted around 332 K inside the adiabatic calorimeter. By applying the so-called fractional melting method, the temperature of fusion of pure compound (calorimetric sample) is obtained as 331.87 K

Table 4 Atomic coordinates and thermal parameters of low-temperature phase of *p*-methylbenzyl alcohol at 100 K

Atom	*x*	*y*	*z*	U_{eq}
C11	0.84895(10)	–0.0190(3)	0.13448(11)	0.0162(3)
C12	0.88621(11)	0.0693(4)	0.22643(10)	0.0194(3)
C13	0.96116(11)	0.2585(4)	0.25010(10)	0.0203(3)
C14	1.00144(11)	0.3631(4)	0.18360(11)	0.0185(3)
C15	0.96365(11)	0.2732(4)	0.09166(10)	0.0189(3)
C16	0.88800(11)	0.0861(4)	0.06753(11)	0.0186(3)
C17	0.77011(11)	–0.2331(4)	0.10648(11)	0.0178(3)
C18	1.08168(12)	0.5716(4)	0.20964(12)	0.0229(4)
O11	0.70156(8)	–0.2158(3)	0.15721(8)	0.0202(3)
C21	0.68311(10)	0.8364(3)	0.46660(10)	0.0155(3)
C22	0.72487(11)	0.7384(4)	0.55683(10)	0.0181(3)
C23	0.80010(11)	0.5492(4)	0.57458(11)	0.0207(3)
C24	0.83552(11)	0.4539(3)	0.50355(12)	0.0187(3)
C25	0.79369(11)	0.5528(4)	0.41348(11)	0.0206(3)
C26	0.71823(11)	0.7416(4)	0.39555(10)	0.0182(3)
C27	0.60341(11)	1.0472(4)	0.44567(10)	0.0165(3)
C28	0.91554(12)	0.2424(4)	0.52323(13)	0.0239(4)
O21	0.54653(8)	1.0381(3)	0.50853(7)	0.0195(3)
C31	0.47897(10)	0.4793(3)	0.18796(10)	0.0149(3)
C32	0.43125(11)	0.5861(4)	0.10017(10)	0.0177(3)
C33	0.35695(11)	0.7741(4)	0.08978(10)	0.0188(3)
C34	0.32730(11)	0.8609(3)	0.16576(11)	0.0175(3)
C35	0.37510(11)	0.7516(4)	0.25322(10)	0.0181(3)
C36	0.44997(11)	0.5648(4)	0.26413(10)	0.0180(3)
C37	0.55871(10)	0.2699(4)	0.20174(10)	0.0168(3)
C38	0.24833(12)	1.0697(4)	0.15415(12)	0.0212(3)
O31	0.60775(8)	0.2831(3)	0.13198(7)	0.0189(2)
H11	0.6747(13)	–0.069(4)	0.1426(13)	0.021(5)
H12	0.8576(12)	–0.008(4)	0.2736(12)	0.022(5)
H13	0.9880(13)	0.324(5)	0.3151(13)	0.028(5)
H15	0.9912(12)	0.344(4)	0.0439(11)	0.019(4)
H16	0.8621(13)	0.035(5)	0.0045(13)	0.024(5)
H171	0.7411(12)	–0.217(5)	0.0420(12)	0.017(4)
H172	0.7997(12)	–0.410(5)	0.1168(12)	0.020(5)
H181	1.0579(15)	0.759(7)	0.2115(15)	0.050(7)
H182	1.1270(16)	0.537(6)	0.2704(16)	0.045(6)
H183	1.1242(17)	0.562(6)	0.1727(17)	0.056(7)
H21	0.5172(17)	0.881(5)	0.5011(18)	0.042(7)
H22	0.7020(12)	0.794(5)	0.6089(12)	0.022(5)
H23	0.8281(14)	0.482(5)	0.6386(13)	0.029(5)
H25	0.8176(12)	0.489(4)	0.3626(12)	0.023(5)
H26	0.6919(12)	0.810(5)	0.3338(12)	0.022(5)
H271	0.6291(12)	1.241(5)	0.4485(12)	0.024(5)
H272	0.5623(12)	1.021(4)	0.3814(12)	0.017(4)
H281	0.8891(15)	0.071(6)	0.5262(14)	0.036(6)

Table 4 Continued

Atom	*x*	*y*	*z*	U_{eq}
H282	0.9483(13)	0.249(5)	0.4745(14)	0.038(6)
H283	0.9670(14)	0.289(5)	0.5820(14)	0.039(6)
H31	0.6354(15)	0.433(4)	0.1421(15)	0.029(6)
H32	0.4523(12)	0.524(5)	0.0436(12)	0.020(5)
H33	0.3213(13)	0.847(5)	0.0276(13)	0.030(5)
H35	0.3583(12)	0.799(4)	0.3092(11)	0.021(4)
H36	0.4816(13)	0.489(4)	0.3243(13)	0.022(5)
H371	0.6041(12)	0.287(5)	0.2633(12)	0.021(4)
H372	0.5309(12)	0.096(5)	0.1969(12)	0.014(4)
H381	0.2740(15)	1.265(6)	0.1509(15)	0.043(6)
H382	0.1949(15)	1.033(5)	0.0993(15)	0.038(6)
H383	0.2247(13)	1.078(5)	0.2071(14)	0.031(5)

Table 5 Hydrogen bonds in low-temperature phase of *p*-methylbenzyl alcohol at 100 K/Å

D–H...A	*d*(D–H)	*d*(H...A)	*d*(D...A)	∠DHA
O11–H11...O31	0.81(2)	1.95(2)	2.7487(18)	168.9(19)
O21–H21...O21_#1	0.86(2)	1.89(2)	2.7524(10)	177(2)
O31–H31...O11_#2	0.82(2)	1.94(2)	2.7586(18)	176(2)

Symmetry transformations used to generate equivalent atoms: #1 $-x+1, y-1/2, -z+1$; #2 $x, y+1, z$

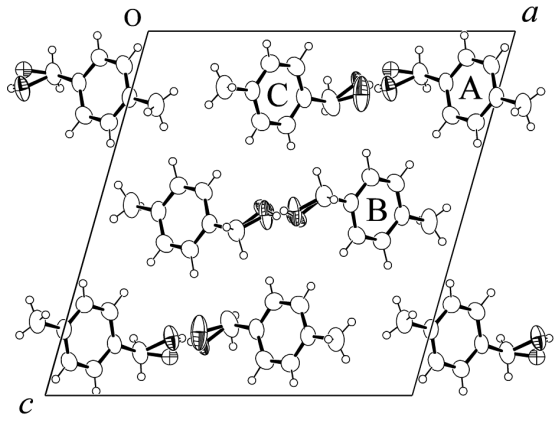

Fig. 2 Crystal structure of the room-temperature phase of *p*-methylbenzyl alcohol obtained by the split atom refinement viewed along the *b*-axis

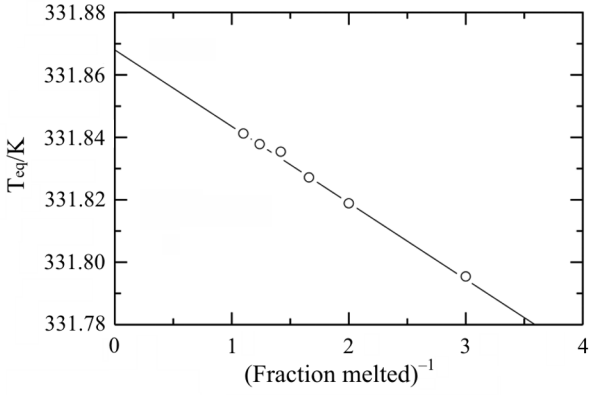

Fig. 3 Equilibrium temperature between solid and liquid phases of *p*-methylbenzyl alcohol as a function of the fraction melted under the adiabatic condition

(331.84 K) as shown in Fig. 3 assuming the liquid-soluble/solid-insoluble impurities. The slope of the straight line in Fig. 3 indicates the purity of the calorimetric sample be 99.95 mol%. The enthalpy and entropy of fusion was determined as (20.170±0.003) kJ mol^{-1} and (60.78±0.01) J K^{-1} mol^{-1}, respectively.

Equilibrium phase transition behavior

Figure 4 shows the results in the first calorimetric run performed routinely without any special criterion concerning the equilibration after cooling down to liquid nitrogen temperature from room temperature. The filled circles depict the temperature drift between about 10 and 15 min after the heater power was turned off. Two sharp dips due to the first-order phase transitions can be seen in accordance with the apparent heat capacity plotted by open circles. Since their location is close to the reported phase transition temperatures, they are ascribed to the successive phase transitions. Beside the dips due to the successive phase transitions, the heat evolution is clearly seen below the lower phase transition. This heat evolution suggests a progress of monotropic phase transition from a super-

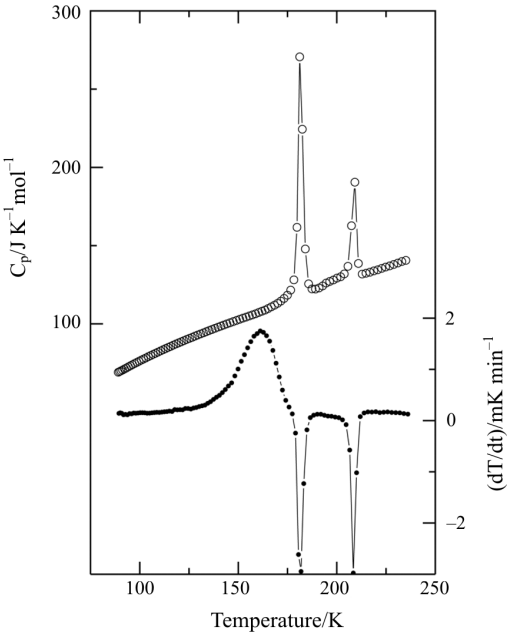

Fig. 4 Heat capacity (left axis and open circle) and temperature drift (right axis and filled circle) of the first calorimetric run on *p*-methylbenzyl alcohol

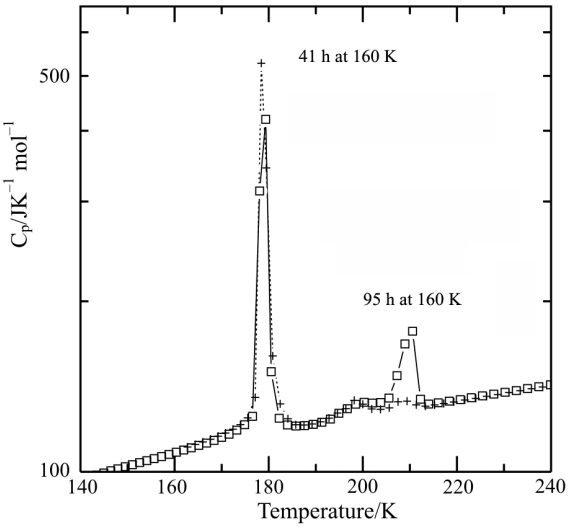

Fig. 5 Effect of the duration of anneal at 160 K. The ordinate is in logarithmic scale

cooled phase to the low-temperature phase. As the heat evolution is maximum around 160 K, long anneal of the sample there for different durations ranging from 8 to 95 h were made.

The apparent heat capacities after anneal are shown in Fig. 5. It is clear that the latent heat of phase transitions around 179 and 210 K largely depends on the duration of anneal. On the other hand, the heat capacities in the vicinity of the transition region remain constant within the experimental precision. In spite of the large change in relative magnitudes, the combined entropy of the LT–IT and IT–RT phase transitions remains ca. 5 J K^{-1} mol^{-1} if two transitions occur. After repeating anneal and measurement cycles, it was concluded that the saturated latent heats are observed if the sample is annealed longer than 60 h. In the course of repeating the experiments, the phase transition temperatures were determined as (179.0±0.5) and (210.0±0.5) K.

Beside the fact that long anneal is necessary for completion of the RT→LT phase transition, a tendency was certainly observed concerning the history dependence of phase transition behavior [6] that the duration of the annealing for stabilization shortens if the sample experienced the transitions. No complete dependence was, however, clarified because a prolonged period is necessary for experiments.

Figure 6 shows the heat capacity result of the well-annealed sample, which is believed being fully stabilized. Heat capacities measured after sufficient anneal are slightly smaller than those without anneal between 100 and 150 K.

Strong history dependence and successful supercooling shown in Fig. 7 demonstrates the first-order nature of these transitions. The enthalpy and entropy of transition were determined from the repeated runs after sufficient anneal as 731 J mol^{-1} and 4.08 J K^{-1} mol^{-1}, respectively, for the lower phase transition at 179 K between the LT and IT phases. They were 206 J mol^{-1} and 0.98 J K^{-1} mol^{-1}, respectively, for the higher transition at 210 K between the IT and RT phases. The properties of phase transitions are summarized in Table 6.

A small step in heat capacity can be recognized in Fig. 5 at 198 K irrespective of duration of anneal. If the fresh sample was cooled from room temperature to 182 K, just above the lower phase transition, a peak in heat capacity was observed around 198 K as shown

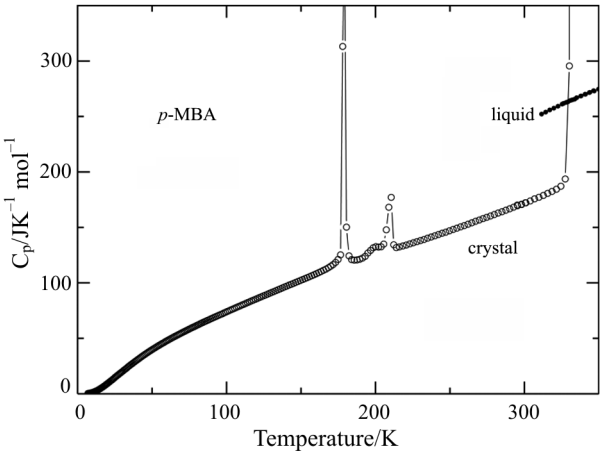

Fig. 6 Heat capacities of the well-stabilized crystal (open circle) and liquid (filled circle) of *p*-methylbenzyl alcohol

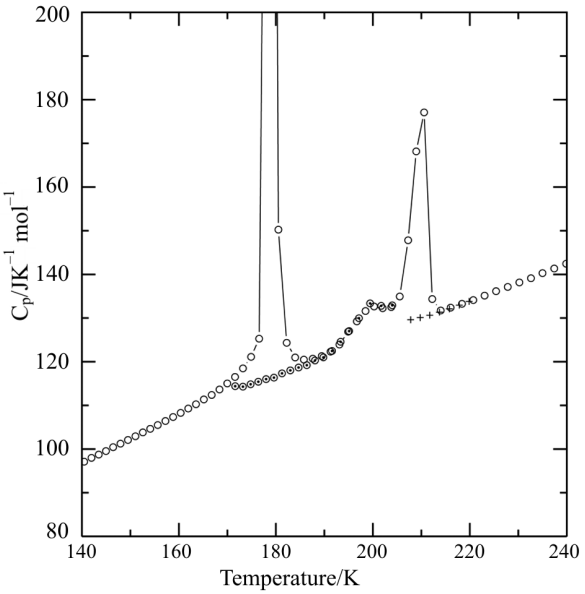

Fig. 7 Supercooling phenomena of the successive phase transitions in crystalline *p*-methylbenzyl alcohol. Results in different calorimetric runs are plotted by different symbols

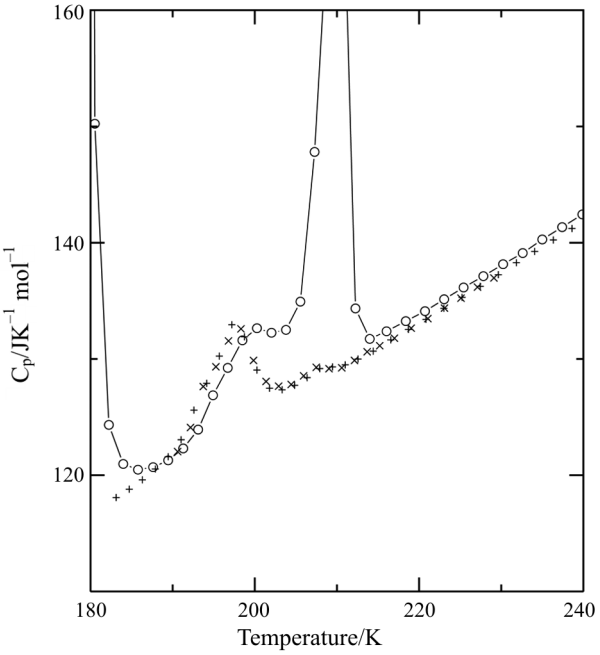

Fig. 8 Heat capacities (crosses and plus signs) of fresh samples of *p*-methylbenzyl alcohol after cooling down just above the lower phase transition temperature. The heat capacity of the well-annealed sample is also shown by open circle for comparison

in Fig. 8. This peak is reproducible, giving the enthalpy and entropy increments of 60 J mol^{-1} and 0.30 J K^{-1} mol^{-1}, respectively. It is interesting that the temperature of peak is close to that of the step in heat capacity in Fig. 5. This can be rationalized if a constant portion of the sample transform to another unknown phase than the LT phase and this unknown phase returns to the RT phase at 198 K.

Standard thermodynamic functions

Heat capacities of the LT and IT phases were measured from 6 K after sufficient anneal. The measured heat capacities thus obtained were smoothed out by least-squares methods and integrated in appropriate ways from low temperatures to yield standard thermodynamic functions. Contributions below the lower temperature limit of the experiment were estimated assuming the Debye model for the lattice vibration. Although the nature of a small peak around 198 K is unknown, the experimental heat capacities were treated as the intrinsic ones. A small contribution of the anomaly was added at 198 K to thermodynamic functions. Resultant thermodynamic functions are tabulated in Table 7 at round temperatures.

Phase transition mechanism

Since the combined entropy of transition depends only weakly on the duration of anneal as described above, the crystal structure of the LT phase determined is sufficient for the discussion on the entropy of transition. Assuming the random mixing, the entropy contributions due to the observed positional disorder detected in the RT phase are calculated according to the Eq. $\Delta S = -R[x\ln x+(1-x)\ln(1-x)]$ as follows:

- Molecule A: 1.8 J K^{-1} mol^{-1}·1/3=0.6 J K^{-1} mol^{-1}
- Molecule B: 5.5 J K^{-1} mol^{-1}·1/3=1.8 J K^{-1} mol^{-1}
- Molecule C: 5.7 J K^{-1} mol^{-1}·1/3=1.9 J K^{-1} mol^{-1}

The resultant sum is ΔS=4.2 J K^{-1} mol^{-1}. The successive phase transition can be said to have a character of an order-disorder transition though partially, if the entropy of transition is comparable to this magnitude.

The combined entropy of successive phase transitions is ca. 5 J K^{-1} mol^{-1}. This is comparable to and larger than the estimated entropy (4.2 J K^{-1} mol^{-1}) from the positional disorder detected in the structure analysis at 250 K in this study. It is therefore con-

Table 6 Properties of phase transitions of *p*-methylbenzyl alcohol

Transition	T_{trs}/K	$\Delta_{trs}H$/kJ mol^{-1}	$\Delta_{trs}S$/J K^{-1} mol^{-1}
LT–IT	179.0±0.5	0.731	4.08
IT–RT	210.0±0.51	0.208	0.98
RT–liquid*	331.868±0.003	20.170±0.003	60.78±0.01

*Pure compound

Table 7 Thermodynamic functions of *p*-methylbenzyl alcohol

$\frac{T}{K}$	$\frac{Cp°}{J\,K^{-1}mol^{-1}}$	$\frac{S°(T)-S°(0)}{J\,K^{-1}mol^{-1}}$	$\frac{[H°(T)-H°(0)]/T}{J\,K^{-1}mol^{-1}}$	$\frac{-[G°(T)-H°(0)]/T}{J\,K^{-1}mol^{-1}}$
Low temperature crystalline phase				
10	1.265	0.31	0.41	0.10
20	9.187	2.51	3.36	0.85
30	20.093	6.55	9.15	2.59
40	30.555	11.26	16.38	5.12
50	39.792	16.07	24.21	8.15
60	47.839	20.71	32.20	11.49
70	54.992	25.10	40.12	15.01
80	61.639	29.26	47.90	18.64
90	67.895	33.21	55.52	22.32
100	73.889	36.98	62.99	26.01
110	79.787	40.60	70.31	29.71
120	85.548	44.11	77.50	33.39
130	91.194	47.51	84.57	37.06
140	96.822	50.83	91.53	40.70
150	102.38	54.09	98.40	44.32
160	108.04	57.28	105.19	47.91
170	114.95	60.46	111.94	51.48
179	122.84	63.39	118.06	54.67
Intermediate temperature crystalline phase				
179	116.45	67.47	122.14	54.67
180	116.90	67.74	122.79	55.05
190	121.37	70.45	129.23	58.78
200	125.84	73.41	135.88	62.47
210	130.31	76.01	142.12	66.11
Room temperature crystalline phase				
210	128.77	76.99	143.11	66.11
220	133.23	79.45	149.20	69.75
230	137.77	81.88	155.22	73.34
240	142.40	84.31	161.18	76.87
250	147.11	86.73	167.09	80.36
260	151.92	89.14	172.95	83.81
270	156.83	91.56	178.78	87.22
280	161.83	93.98	184.57	90.60
290	166.94	96.40	190.34	93.93
300	172.16	98.84	196.09	97.24
310	177.50	101.29	201.82	100.53
320	182.93	103.76	207.54	103.78
330	188.49	106.24	213.25	107.01
331.87	189.55	106.71	214.32	107.61
Liquid				
331.87	264.92	112.79	220.40	107.61
340	269.49	116.48	226.87	110.39
350	274.71	120.93	234.75	113.83
Room temperature crystalline phase				
298.15	171.18	98.39	195.02	96.63

cluded that the successive phase transitions of *p*-MBA has a character of an order-disorder phase transition. It is noted that the observed disorder is not related to the symmetry. The degree of disorder can be reduced on decreasing temperature. There exists in the entropy of transition a contribution of vibrational

entropy, of which the magnitude is expected small because of the resemblance of crystal structures of the RT and LT phases. In order to divide firmly the entropy of transition into two contributions, configurational disorder and (lattice) vibration, the precise structure analysis just above the transition temperature is necessary.

It is easiest to imagine a double-well potential assumed in the NMR study [2, 6] for the proton (deuteron) in hydrogen bond being related to the fact that there are two potential minima along the bond. The positional disorder detected in this study is, however, not of hydrogen but of oxygen atom. The interpretation on the NMR results rely only little on geometrical parameters. If there exists two states that are energetically nonequivalent to each other and they are responsible for the nuclear magnetic relaxation, they would be well described by the double-well potential model. The detected disorder of oxygen atom in OH group is certainly compatible with the NMR results [6].

There still remains an issue to be considered. That is, why is there the IT phase between the LT and RT phases. Due to experimental difficulty arising from the first-order nature of the higher transition, complete structure determination of the IT phase was unsuccessful as described briefly. Although the entropy contribution of each chain (chain B and A–C) is comparable to the entropy of the higher transition, it is hard to imagine such separate ordering while considering similar two-step phase transitions in *p*-XBA [1–5], where only one type of chain exists. Elaborate experiments will be necessary while taking the necessity for long anneal observed in this study into account.

Conclusions

Crystal structures of the room-temperature (RT) and low-temperature (LT) phases of *p*-MBA were reexamined by single-crystal X-ray diffraction method. In the RT phase at 250 K, positional disorder of the oxygen atoms in OH bonds was certainly detected in contrast to the previous structure report. The contribution of this disorder is roughly estimated as ca. 4 $J\,K^{-1}\,mol^{-1}$ to the combined entropy of transition. The structure of the LT phase coincided to the previous one. Heat capacities were measured by adiabatic calorimetry between 6 and 350 K on a high purity sample (99.95mol% determined by cryometry at its melting temperature, 331.87 K). The structural phase transitions of first-order were observed at 179 and 210 K and require long time (about 60 h for bulk sample) for completion. The combined entropy of transition was ca. 5 $J\,K^{-1}\,mol^{-1}$. Comparison of experimental and calculated entropies of transition shows that the successive phase transition in *p*-MBA has a character of an order-disorder phase transition. Standard thermodynamic functions are tabulated for the stable phase sequence, LT crystalline phase – IT crystalline phase – RT crystalline phase – liquid, below 350 K.

References

1 M. Hashimoto, Y. Nakamura and K. Hamada, Acta Crystallogr. Sect. C, 44 (1988) 482.
2 M. Mizuno, M. Hamada, T. Ida, M. Suhara and M. Hashimoto, Z. Naturforsch., 57 (2002) 388.
3 M. Hashimoto and A. Weiss, Ber. Bunsenges. Phys. Chem., 86 (1982) 134.
4 H. Niki, K. Kano and M. Hashimoto, Z. Naturforsch., 51 (1996) 731.
5 M. Hashimoto, Y. Monobe, H. Terao, H. Niki and K. Mano, Z. Naturforsch., 53 (1998) 436.
6 M. Hashimoto, M. Harada, M. Mizuno, M. Hamada, T. Ida and M. Suhara, Z. Naturforsch., 57 (2002) 381.
7 SAINT (Ver. 6.45), Bruker AXS Inc., Madison, Wisconsin, USA (2003).
8 G. M. Sheldrick, SADABS, University of Göttingen, Germany (1996).
9 SHELXTL (Ver. 6.14), Bruker AXS Inc., Madison, Wisconsin, USA (2003).
10 L. J. Farrugia, J. Appl. Cryst., 30 (1997) 565.
11 Y. Yamamura, K. Saito, H. Saitoh, H. Matsuyama, K. Kikuchi and I. Ikemoto, J. Phys. Chem. Solids, 56 (1995) 107.

DOI: 10.1007/s10973-005-7072-2